https://doi.org/10.48048/tis.2022.3200

Increasing the Sensitivity of Polymer Optical Fiber Sensing Element in Detecting Humidity: Combination of Macro and Micro Bendings

Heru Kuswanto, Ichwan Abimanyu and Wipsar Sunu Brams Dwandaru*

Department of Physics Education, Faculty of Mathematics and Natural Sciences, Universitas Negeri Yogyakarta, Yogyakarta 55281, Indonesia

(*Corresponding author's e-mail: wipsarian@uny.ac.id)

Received: 6 November 2020, Revised: 30 May 2021, Accepted: 6 June 2021

Abstract

Humidity sensing is essential in various fields, including industrial processes, agriculture, engineering, and health. A material suitable as a sensing element for humidity detecting is polymer optical fiber (POF). In this study, a combination of micro and macro bendings was proposed to increase the sensitivity of the sensing element. The sensing element was constructed by peeling the out-most coating of the POF, but keeping intact the cladding and core. The macro bending was done upon the peeled part of the POF by making a circular form with varying diameter of 3.5, 4.0 and 4.5 cm. The micro bending was constructed by making a local bent via subjecting to electrical discharge flame from an inductor generator with varying number of micro bendings, i.e., 1, 2 and 3. The sensing element was then tested for its sensitivity as a humidity sensor. The sensing element was positioned inside a self-custom made humidity measurement box consisting of a hygrometer and a pipe to stream water vapor inside the box. The normalized power was measured by varying the % humidity inside the box. In general, the result showed that increasing the humidity caused the normalized lupower to decrease, hence increasing the power loss of the sensing element. Moreover, the sensitivity of the sensing element was increased 10 times for the combined micro and macro bendings compared to a sensing element without micro bendings.

Keywords: Polymer optical fiber, Humidity sensor, Macro bending, Micro bending, Sensitivity

Introduction

Humidity control is an important element for maintaining a healthy environment in houses or factories. Humidity affects the health and air quality of buildings and their inhabitants. It even supports manufacturing performance to run optimally. Industrial processes, agriculture, civil engineering, and structural health monitoring are strongly influenced by humidity [1,2]. Moreover, condensation on the surface encourages corrosion or mold growth. Hence, the availability of humidity measurement devices is therefore essential in order to determine and control the humidity level of the environment. Conventional humidity measurement utilizes mechanical and electrical effects, such as mechanical hygrometer, chilled mirror hygrometer, wet and dry bulb psychrometer, and infrared (IR) optical absorption hygrometer [3]. There are various methods in constructing humidity measurement devices, i.e., humidity sensors based on 1) optical absorption, 2) gratings, which consists of fiber Bragg and long period fiber gratings, 3) interferometry, e.g., Fabry-Perot, Sagnac, and modal interferometers, 4) resonators, e.g., microloop, microring, microtoroid, and microsphere, and 5) electromagnetic resonances, especially lossy mode resonances [1,2]. The aforementioned sensing methods have their own advantages, and therefore utilized according to the intended applications, e.g., humidity measuring devices based on induced-stress-optic effect [4], agarose gel [5,6], evanescent wave scattering [7], liquid-level measurement for industrial application [8,9], and displacement sensors [10].

Humidity measurement using optical fibers (OF) is a potential alternative as it has many advantages, such as small size [11,12], bio-compatible [13], has remote sensing ability [4], free of electromagnetic interference [2], and can withstand impacts and vibrations [14]. In general, there are 2 types of OF, viz.: Glass and polymer optical fiber (POF). POF is more superior compared to glass fiber optic, such as bigger core diameter, higher flexibility, lighter weight, easier to be coupled, and cheaper [15]. Moreover, POF can be handled without special equipment or technique, and easy to be used by

anyone without special training. Especially in this study, POF is very suitable for low-speed and short distance applications, such as humidity measurement sensors [16]. POF may be applicable to housing networks and appliances, industries, or even in transportations. One advantage of the POF that is explored further is its high flexibility. Hence, making POF easily bent. The bending may be circular with certain diameter and/or smaller (local) bent forms known as macro- and micro bendings, respectively. Macro bending the POF has been utilized as the sensing element for humidity sensors, e.g., see [15,17,18] via producing power loss upon the POF.

The characteristics of power loss of POF sensors have been studied in various literatures. Experimental and numerical studies have been conducted in order to study a sensing element based on bending and elongated grooved of the POF [15]. Cheng *et al*. [19] have studied the macro bending loss of POF utilized for crack opening displacement. A correspondence between the geometry of helical structure and macro bending loss of POF for monitoring pavement loss is explored in [20]. The bending treatment effect shows that reducing the bending radius increases the power loss [21]. The significant increase in the power loss due to the POF bending is dependent upon various parameters such as the refractive index [22], bending radius [23,24], and wavelength of the light sources [15]. Moreover, adding a local or micro bending on the POF gives a significant effect towards the additional increase of power loss, which is induced when humidity of the environment changes. Hence, a combination of macro and micro bendings is further explored upon the POF for humidity sensor based on power loss.

The sensing principle of the POF proposed here can be explained by the macro bending effect of the POF. When a POF is bent at a location, then optical power loss is induced at that location. The mechanism behind the bending loss is explained by considering that the refractive index of the cladding is lower than that of the POF core. For a straight POF (without bending), a light that is launched into the core at a low angle measured from its axis undergoes total internal reflection between the core and cladding interface. However, when the POF is bent some of the light escapes from the core and cladding due to the change of the incidence angle. This loss is given by a formula given as follows [14];

$$\text{Loss} = \frac{T}{2\sqrt{R}} \exp\left(2Wa - \frac{2W^3}{3\beta^2} R\right), \tag{1}$$

with $T = \frac{2ak^2}{e\sqrt{\pi W}V^2}$, $W^2 = \beta^2 - n_2^2 k_0^2$, $V^2 = a^2 k_0^2 (n_1^2 - n_2^2)$, a is the radius of the core fiber, R is the radius of the bend, $k = \frac{2\pi}{\lambda}$, $k_0 = \frac{2\pi}{\lambda_0}$, T is the total of birefringence fiber effect, β is the phase constant, n_1 is the refractive index of the core, and n_2 is the refractive index of the cladding. Eq. (1) shows that there is a critical curvature radius. If the curvature radius is larger than the critical curvature radius, then there is no loss of power. On the other hand, if the curvature radius is smaller than this critical curvature radius, then there is optical loss. Furthermore, the variation in the refractive index (n) of these POF bendings with respect to humidity (H) is obtained from Lorenz-Lorentz relation as [11];

$$\frac{dn}{dH} = \frac{(n^2+2)^2}{6n} k_m S \left(1 - \frac{f}{f_c}\right), \tag{2}$$

where k_m is the molar refraction divided by the molecular weight of water, S is the moisture solubility of the polymer, $f(0 < f < 1)$ is the fraction of the absorbed moisture that contributes to an increase in polymer volume, and is expected to depend on temperature. In Eq. (2) the critical value, f_c, is defined by $f_c = k_m \rho_m \frac{n_p^2+2}{n_p^2-1}$, where n_p is the refractive index of the polymer without any moisture and ρ_m density of water. Finally, the output power (P_{out}) of the POF sensor head with respect to n of the sensing layer is given by;

$$P_{out} = P_{in} \left(\frac{n_1^2 - n^2}{n_1^2 - n_2^2}\right), \tag{3}$$

where P_{in} represents the total power injected into the guided modes of the POF from the source.

Materials and methods

The POF used in this study is SH-4001 produced by Mitsubishi Rayon Company Ltd. The POF is specified with coating diameter of 2.2 mm, cladding diameter of 1 mm, and core diameter of 0.98 mm

with a numerical aperture of 0.5. The materials of the core and cladding are polymethyl methacrylate (PMMA), polytetrafluoroethylene (PTFE), and low-density polyethylene (LDPE). The core refractive index is 1.492 and cladding refractive index is 1.402. Moreover, the equipment used in this study is an induction generator (**Figure 1(a)**), a hygrometer, an optical power meter (OPM), and a knife. The light source utilized in this study is Helium-Neon (He-Ne) laser with a wavelength of 632.8 nm as a light source for the POF. Finally, a self-custom made plastic box for humidity measurement is constructed (**Figure 1(b)**).

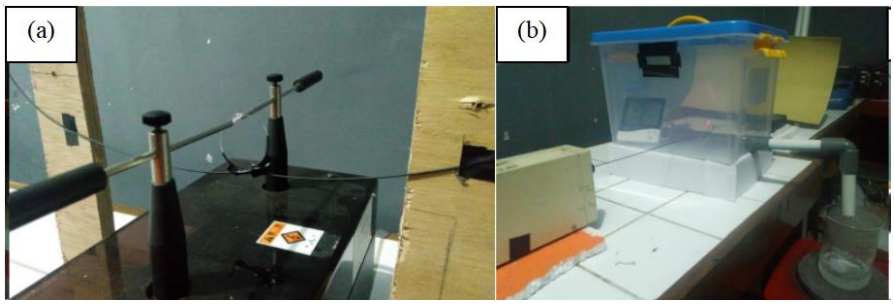

Figure 1 The equipment used, e.g., (a) an induction generator and (b) a self-custom made humidity measurement box.

In order to produce the macro bending, the out-most coating of the POF is mechanically peeled off using a knife such that the remaining materials are only the cladding and the core. The length of the peeled (out-most) coating is varied with values of 4, 6, and 8 cm. The peeled part of the POF is then bent into a circular form, which signifies the macro bending. Because the length of the peeled coating is varied then the diameter of the bending is also varied, i.e., the longer the peeled coating the longer the diameter of the bending (see **Figure 2**).

Table 1 shows the variation of the macro bending diameters and number of micro bendings. The diameter variations used in this study are 3.5, 4.0, and 4.5 cm. Each macro bending diameter variation is given 3 variation of the micro bending, i.e., 1, 2, and 3. Hence, there are 9 variations of POF as the sensing elements for humidity detection. **Figures 2(a)** to **2(e)** corresponds to fiber codes of C3, C2, B3, A3, and A1, respectively.

Table 1 Variation of diameter and indentation.

No.	Fiber code	Macro bend diameter (cm)	Number of micro bend
1	A1	3.5	1
2	A2	3.5	2
3	A3	3.5	3
4	B1	4.0	1
5	B2	4.0	2
6	B3	4.0	3
7	C1	4.5	1
8	C2	4.5	2
9	C3	4.5	3

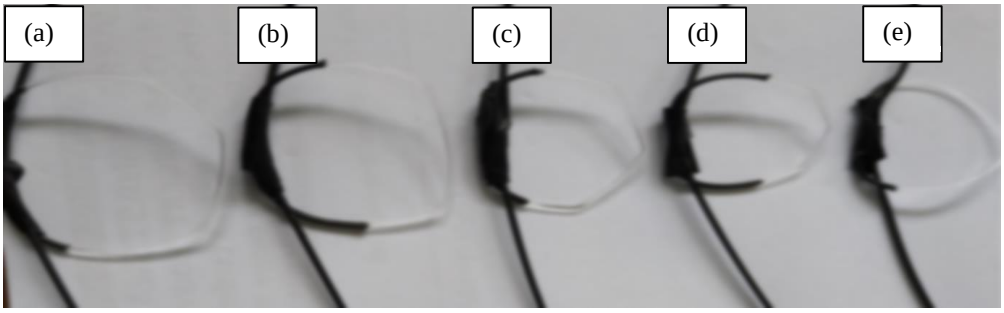

Figure 2 Macro and micro bendings of POF with code specifications given in **Table 1**, i.e., (a) C3, (b) C2, (c) B3, (d) A3, and (e) A1.

The micro bending is produced by giving a small or local bent upon the POF using an induction generator (**Figure 1(a)**). The bent is formed due to the effect of the discharge flame between 2 electrodes on the induction generator. The distance between 2 electrodes is 8 mm. The part of the POF, especially the circular (macro bend) part, to be locally bent is placed in middle of the 2 electrodes. The micro bent is formed after being hit by the flame produced by the induction generator for 30 s. **Figure 2** shows the results of the POF with various combinations of macro and micro bendings.

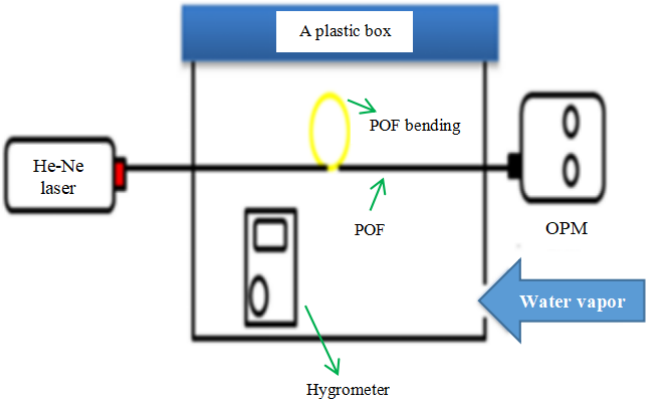

Figure 3 The data collection scheme.

The sensing elements of the POF that have been given macro and micro bendings are then tested as humidity sensors. **Figure 3** shows the data collection scheme to determine the effect of the bendings towards the changes in the humidity. The apparatus on **Figure 3** is a self-custom made humidity measurement box (**Figure 1(b)**). This apparatus consists of a big plastic box. Inside the box, the sensing elements are set across the box from one end to the other end of the box. A hygrometer as a detector for humidity is also placed inside the box. Water vapor may be streamed into the box to vary the humidity inside the box. Every change in the humidity is compared to the attenuation of light intensity read by the OPM. The range of humidity percentage (% humidity) is 60 to 75%.

Results and discussion

The micro bending upon the POF may be observed in **Figure 4** using a light microscope. The micro bending is in the form of a sharp and local indentation on the POF (yellow arrow). It may be observed that the bending part is smooth and does not look to be damaged from the flame induction treatment. The bending increases in **Figures 4(a)** - **4(c)**. A white light passes through the bent POF in **Figures 4(a)** and **4(b)**. The existence of this micro bending causes a change in the path of light passing through the POF, i.e., from a path with an angle greater than the critical angle to a path with an angle lower than the critical angle. Hence, causing some of the light rays to escape the POF and thus producing the power loss. If this bending increases, the power loss also increases, which is consistent with the study in [21].

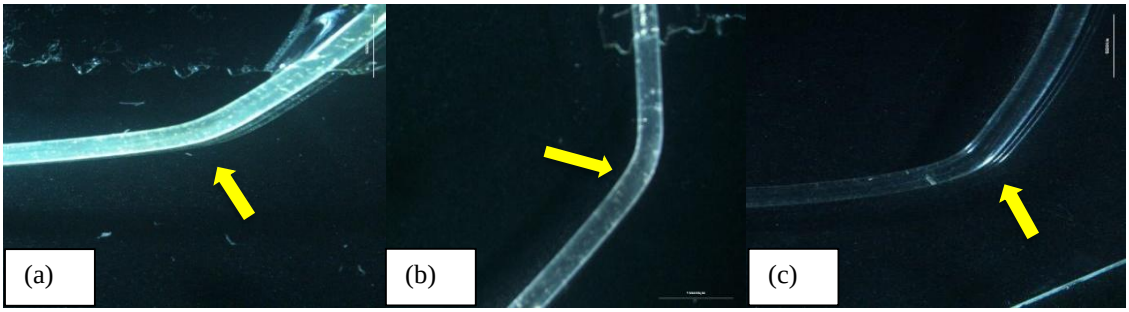

Figure 4 The micro bending upon the POF magnified 10× using a light microscope. The yellow arrow is the local bending on the POF.

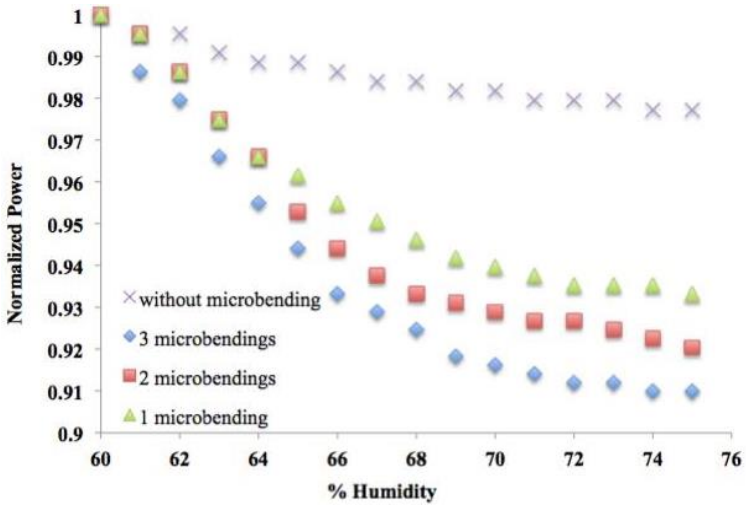

Figure 5 The normalized power vs % humidity for the sensing element with varying number of micro bendings (and a macro bending).

The normalized power loss of the POF as a function of the humidity (%) can be observed in **Figure 5** with variation of the number of micro bendings. In this case, the macro bending is set to be constant with a diameter of 4 cm. The data in the forms of crosses, triangles, rectangles, and diamonds represent the normalized power loss of the POF with 0, 1, 2 and 3 micro bendings, respectively. In general, it may be observed that increasing the humidity causes the power loss to increase (i.e., the normalized power decreases). This means that the change in humidity affects the normalized power of the POF having micro and macro bendings. This is in accordance with the result in [7] where a relative humidity sensor using tapered POF coated with seeded Al-doped ZnO is studied producing a decrease in the output voltage as the relative humidity is increased. A study in [1] on humidity sensing using PMMA POF also produces decreasing backscatter intensity change, which is decreasing as the relative humidity is increased. However, on the contrary, a study in [25] concerning relative humidity sensor based on evanescent-wave POF shows an increase of fiber output as the relative humidity is increased. It may also be observed that there is a difference between the normalized power decrease (as the humidity is increased) graphs between the POF without and with micro bendings (for all number of micro bendings), i.e., the normalized power drops when the POF is given micro bendings. The normalized power decreases further as the number of micro bendings is increased.

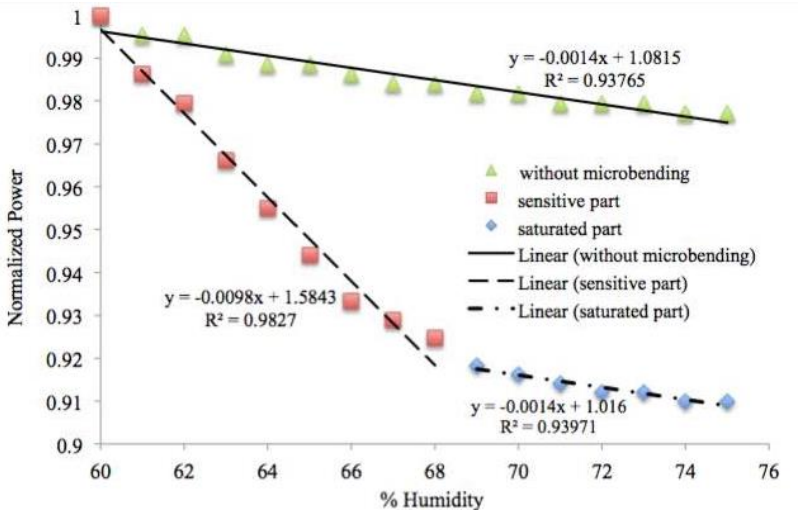

Figure 6 Sensitivity of the humidity sensing using POF without and with 2 micro bendings.

A further inspection of the normalized power decrease of the POF with micro bendings (as the humidity is increased) is that the profiles have linear trends at the beginning, i.e., at 60% humidity, and tend to saturate after a certain humidity value. Hence, 2 of the profiles from **Figure 5** are further observed, which are the profiles without and with 2 micro bendings. Linear trendlines are produced for these 2 profiles given in **Figure 6**. The linear trendline of the profile without micro bending is given as follows (black solid line in **Figure 6**);

$$y = -0.0014x + 1.0815. \quad (4)$$

Moreover, the linear trendlines of the profile with 2 micro bendings are divided into 2 parts, i.e., the sensitive and the saturated parts, given by (black dashed-lines in **Figure 6**);

$$y = -0.0098x + 1.5843, \quad (5)$$

and

$$y = -0.0014x + 1.016. \quad (6)$$

It may be observed that the trend line for the normalized power without micro bending is quite slant and the humidity may ranged from 60 to 75%. Hence, the sensor without micro bendings has a sensitivity of about 0.0014/1 %. On the other hand, the linear trend line of the normalized power with 2 micro bendings of the sensitive part is more sharply inclined compared to the linear trendline without micro bendings. In this part, the sensitivity of the POF as a sensing element increases to around 0.01/1 %, i.e., an increase of 10× compared to the sensitivity of the POF without micro bendings. However, the range at this level of sensitivity decreases to around 70% (from 60%). Furthermore, in the saturated part, the trendline becomes similar to the trend line without micro bending with the same value of sensitivity. This means that when the sensor becomes saturated the sensitivity decreases. This analysis is in accordance to that conducted in [15] where they produce the sensitivity of the sensing element with respect to the deformation displacement.

Finally, the diameter of the macro bending is varied and the number of the micro bending is kept constant (3 micro bendings) given in **Figure 7**. The figure shows graphs of normalized power vs % humidity with varying macro bending diameters of 3.5, 4.0, and 4.5 cm, represented by the yellow-triangle, red-rectangular, and blue-diamond data, respectively. It may be clearly observed that decreasing the diameter of the macro bending tends to increase the power loss of the sensing element, which is in accordance with the result in [21]. The greatest power loss is produced by the macro bending diameter of 3.5 cm.

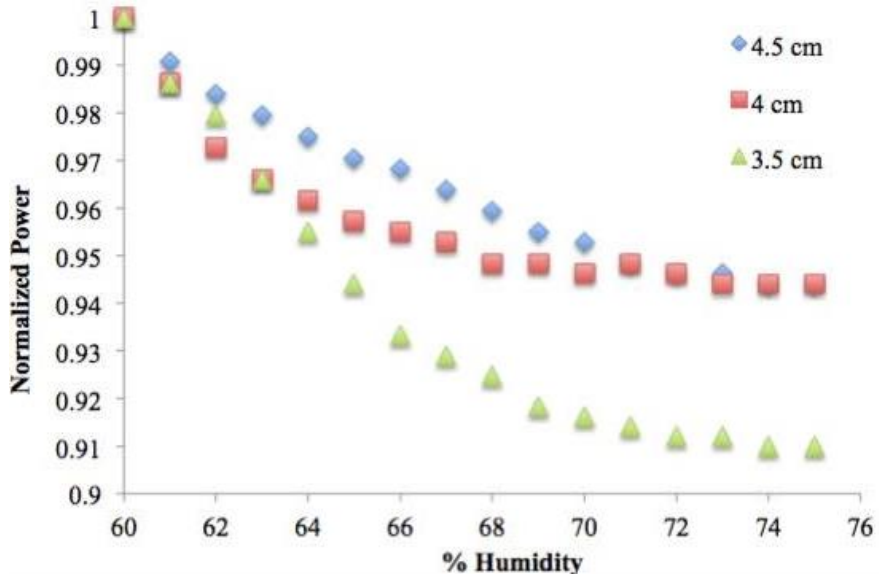

Figure 7 The normalized power vs % humidity for varying macro bending diameters.

One-way to theoretically discuss the relationship between the micro and macro bendings, the power loss, and the humidity of the sensing element is to invoke again Eqs. (1) and (2). In this case we only consider the effect of the loss and the humidity solely by the refractive index of the core and cladding. Modifying Eq. (1) by expanding the exponential term in the RHS of the equation using the power series, and keeping just the first-order term, we obtain;

$$\text{Loss} = \frac{T}{2\sqrt{R}}. \tag{7}$$

Assuming further that $\beta > n_2(k_o)^2$, we produce a proportionality,

$$\text{Loss} \sim \frac{1}{(n_1^2 - n_2^2)}. \tag{8}$$

This means that the loss is inversely quadratic to the refractive index of the core and cladding, i.e., if the refractive index of the core and cladding decreases then the loss increases. Next, Eq. (2) is discussed. It can be observed that $C \equiv k_m S\left(1 - \frac{f}{f_c}\right) \geq 0$, then $dn/dH \geq 0$ because $n > 0$. This means that increasing H increases n, and further relating this to Eq. (8), increasing H means the (power) loss decreases, which is inconsistent with the results obtained in **Figures 5** and **7**. Therefore, a modification of Eq. (2) is given to incorporate the micro and macro bending factors that significantly change the character of dn/dH. The bending of the POF is similar to a peak or a sharp turn of a line (see an illustration of von-Mises stress contours in [15]). A peak or a sharp turn on a line is continuous but not differentiable. Hence, in order to include the latter property, a negative factor in the RHS of Eq. (2) is proposed that constitutes the bendings of the POF, i.e.;

$$\frac{dn}{dH} = -C(a, N)k_m S\left(1 - \frac{f}{f_c}\right)\frac{\left(n^2+2\right)^2}{6n}, \tag{9}$$

with N is the number of the micro bendings. Because of the negative sign in Eq. (9), n decreases as the humidity is increased. This causes the loss to increase as the humidity is increased in accordance with the results of **Figures 5** and **7**.

Conclusions

Micro and macro bendings of POF have been combined as a sensing element in order to increase the sensitivity of the humidity sensor. The micro and macro bendings affect the normalized power of the sensing element in detecting the humidity, i.e., increasing the % humidity tends to decrease the normalize power, hence increasing the power loss. Increasing the number of the micro bendings (and keeping the diameter of the macro bending constant) causes the decrease of the overall profile of the normalized power, and hence increasing the power loss. Moreover, decreasing the diameter of the macro bending tends to decrease the normalized power. It is also demonstrated that the sensitivity of the sensing element increases as it is given a combination of micro and macro bendings compared to the sensing element without micro bending. However, the % humidity range of the sensitive part decreases for the sensing element with combined micro and macro bendings compared to the sensing element without micro bendings. A theoretical aspect of this study is also briefly discussed through a modification on dn/dH by considering a negative factor that depends upon the diameter of the macro bending and the number of micro bendings. A further study may be conducted to observe the physical and chemical properties of the combined micro and macro bendings via various characterizations, e.g. scanning electron microscope (SEM). It is also interesting to study the spectral response of the sensor as well.

Acknowledgements

We would like to thank the Faculty of Mathematics and Natural Science, Universitas Negeri Yogyakarta Indonesia in supporting this research.

References

[1] J Ascorbe, JM Corres, FJ Arregui and IR Matias. Recent developments in fiber optics humidity sensors. *Sensors* 2017; **17**, 893.
[2] S Liehr, M Breithaupt and K Krebber. Distributed humidity sensing in PMMA optical fibers at 500 nm and 650 nm wavelengths. *Sensors* 2017; **17**, 738.
[3] TL Yeo, T Sun and KTV Grattan. Fibre-optic sensor technologies for humidity and moisture measurement. *Sensor. Actuator. A Phys.* 2008; **144**, 280-95.
[4] A Leal-Junior, A Frizerra-Neto, C Marques and MJ Pontes. Measurement of temperature and relative humidity with polymer optical fiber sensors based on the induced stress-optic effect. *Sensors* 2018; **18**, 916.
[5] M Batumalay, SW Harun, F Ahmad, RM Nor, NR Zulkepely and H Ahmad. Study of a fiber optic humidity sensor based on agarose gel. *J. Mod. Optic*. 2013; **61**, 244-8.
[6] L Xu, JC Fanguy, K Soni and S Tao. Optical fibre humidity sensor based on evanescent wave scattering. *Optic. Lett*. 2004; **29**, 1191-3.
[7] J Mathew, KJ Thomas, VPN Nampoori and P Radhakrishnan. A comparative study of fiber optic humidity sensors based on Chitosan and Agarose. *Sensor. Transducers J.* 2007; **84**, 1633-40.
[8] DS Monteroand and C Vazquez. Polymer optical fiber intensity-based sensor for liquid-level measurements in volumetric flasks for industrial application. *Sensor Networks*. 2012; **2012** ,618136,
[9] N Arumnika and H Kuswanto. The influence of curvature configuration on the characteristic of alcohol gel insertion jacket of polymer optical fiber liquid level sensor. *J. Phys. Conf. Ser.* 2018; **1011**, 012053.
[10] J Zhao, T Bao and T Kundu. Wide range fiber displacement sensor based on bending loss. *J. Sensor*. 2016; **2016**, 4201870.
[11] P Wang, K Ni, B Wang, Q Ma and W Tian. Methylcellulose coated humidity sensor based on Michelson interferometer with thin-corefiber. *Sensor. Actuator. A Phys.* 2019; **288**, 75-8.
[12] Z Guo, F Chu, J Fan, Z Zhang, Z Bian, G Li and X Song. Study of macro-bending biconical tapered plastic optical fiber for relative humidity sensing. *Sensor. Rev*. 2018; **39**, 352-7.
[13] M Hernaez, B Acevedo, AG Mayes and S Melendi-Espina. High-performance optical fiber humidity sensor based on lossy mode resonance using a nanostructured polyethylenimine and gaphene oxide coating. *Sensor. Actuator. B Chem*. 2019; **286**, 408-14.
[14] Z Harith, M Batumalay, N Irawati, SW Harun, H Arof and H Ahmad. Relative humidity sensor employing tapered plastic optical fiber coated with seeded Al-doped ZnO. *Optik* 2017; **144**, 257-62.
[15] WH Lu, LW Chen, WF Xie and YC Chen. A sensing element based on a bent and elongated grooved polymer optical fiber. *Sensors* 2012; **12**, 7485-95.

[16] S Muto, O Suzuki and TA Amano. Plastic optical fibre sensor for real-time humidity monitoring. *Meas. Sci. Tech*. 2003; **746**, 746-50.
[17] Z Guo, F Chu, J Fan, Z Zhang, Z Bian, G Li and X Song. Study of macro-bending biconical tapered plastic optical fiber for relative humidity sensing. *Sensor. Rev*. 2019; **39**, 352-7.
[18] W Chen, Z Chen, Y Zhang, H Li and Y Lian. Agarose coated macro-bend fiber sensor for relative humidity and temperature measurement at 2 μm. *Opt. Fiber Tech*. 2019; **50**, 118-24.
[19] L Cheng, Y Li, Y Ma, M Li and F Tong. The sensing principle of a new type of crack sensor based on linear macro-bending loss of an optical fiber and its experimental investigation. *Sensor. Actuator. A Phys*. 2018; **272**, 53-61.
[20] L Meng, L Wang, H Xiong, H Wang and X Guo. An investigatin in the influence of helical structure n bend loss of pavement optical fiber sensor. *Optik* 2019; **183**, 189-99.
[21] J Zubia and J Arrue. Plastic optical fibers: An introduction to their technological processes and applications. *Opt. Fiber Tech*. 2001; **7**, 101-40.
[22] T Watanabe, N Ooba, Y Hida and M Hikita. Influence of humidity on refractive index of polymers for optical waveguide and its temperature dependence. *Appl. Phys. Lett*. 1998; **72**, 1533-5.
[23] X Xing, J Zhang, L Wang, J Pei and X Chen. Effects of bending radius and fiber-crack angle on polymer optical fiber loss for potential application in pavement crack monitoring. *J. Test. Eval.* 2021; **49**, 96-108.
[24] B Lustermann, BM Quandt, S Ulrich, F Spano, RM Rossi and LF Boesel. Experimental determination and ray-tracing simulation of bending losses in melt-spun polymer optical fibres. *Sci. Rep*. 2020; **10**, 11885.
[25] SK Khijwania, KL Srinivasan and JP Singh. An evanescent-wave optical fiber relative humidity sensor with enhanced sensitivity. *Sensor. Actuator. B Chem*. 2005; **104**, 217-22.